Real-Time Model-Adaptive Relaying Applied to Microgrid Protection

Maximiliano Ferrari[1], Travis Smith[2], Neil Shepard[1], Aditya Sundararajan[1], Drew Herron[1] , Emilio Piesciorovsky[1], Isabelle Snyder[1], Ben Ollis[1], Josh Hambrick[3], Chris Sticht[4], Mike Marshall[2]

[1]Oak Ridge National Laboratory, Oak Ridge, TN, USA. [2]DRG Technical Solutions, Columbia, SC, USA.
[3]Open Energy Solutions, Santa Clara, CA, 95054, [4]Idaho National Laboratory.

***Abstract*— In microgrids, the short-circuit current magnitude is significantly limited by more than an order of magnitude due to the relatively small inverter-based resources. Commercially available protective devices for distribution cannot reliably protect a microgrid due to their dependence on the magnitude of the fault current. Moreover, overcurrent relays typically cannot function properly for a microgrid because they are incapable of detecting faults and/or performing the coordination between the relays in inverter-based microgrids operated in the islanded mode. This paper proposes a model-adaptive relay designed to adjust the relay curves based on the available generation and the network topology. The proposed method runs a real-time model of the microgrid, which gathers information from the network to calculate the available short-circuit current in the specified node. The fault current from the model is then used for the adaptive algorithm to calculate the relay settings, considering coordination with the downstream fuses and upstream reclosers. This work presents the validation of the proposed method in Hardware-in-the-Loop, in a hardware testbed as well as field deployed in a real microgrid in East-Tennessee.**

***Index Terms*—Adaptive relay, microgrid protection**

I. Introduction

The ability of microgrids to work independently from the main grid makes them a resilient system because they can power local loads when the main grid is unavailable. However, this resilience is lost if the microgrid is not properly protected during short-circuit faults that occur within its own boundaries [1]. Commercially available protective devices for distribution, such as reclosers, relays and fuses, are typically not suitable for microgrid protection due to the dependence of these devices on the magnitude of the fault current [2]. Traditional overcurrent relays typically cannot function properly for a microgrid because they are incapable of detecting faults and/or performing the coordination between the relays in inverter-based microgrids operated in the islanded mode [3,4].

In microgrids, the short-circuit current drastically changes between grid-tied versus islanded operation [1], [5]. For example, during grid tied operation, the short circuit current ratio of an urban microgrid at the PCC is between 10-50 p.u. the nominal microgrid load current. For a microgrid based on inverter-based generation, the fault current is between 1.2-2.0 p.u. [6-7].

ACKNOWLEDGEMENT Research sponsored by the Laboratory Directed Research and Development Program of Oak Ridge National Laboratory, P.O. Box 2008, Oak Ridge, Tennessee 37831-6285; managed by UT Battelle, LLC, for the U.S. Department of Energy. This manuscript has been authored by UT-Battelle, LLC, under contract DE-AC05- 00OR22725 for the U.S. Department of Energy. The United States Government retains and the publisher, by accepting the article for publication, acknowledges that the United States Government retains non-exclusive, paid-up, irrevocable, worldwide license to publish or reproduce the published form of this manuscript, or allow others to do so, for United States Government purposes. This material is based upon work supported by the U.S. Department of Energy's Office of Energy Efficiency and Renewable Energy (EERE) under the Solar Energy Technologies Office Award Number DE-EE0002243-2144

Such a large difference makes coordination of existing distribution protection based principally on overcurrent devices very difficult and often unattainable [1]. Fuses are particularly affected because of their inverse characteristics; in some cases, fuses protecting the laterals will not clear faults during islanded operation [8].

Adaptive protection is a promising technique that enables the use of overcurrent relays in microgrids. Adaptive protection can be defined as an online process which modifies the preferred protective responses and correlates them to a change in system conditions or requirements in a timely manner through control or signaling [9]. Table I shows a summary for the different approaches in Adaptive Relaying, which can be broadly categorized in centralized, decentralized, or hybrid approaches [10-14]. The central approach uses a central unit to monitor the state of the system and reconfigures the relays to adjust the tripping time. The decentralized approach utilizes local information, such as frequency and voltage, to identify the microgrid status and adapt the relay settings accordingly. Hybrid approaches use a central controller to identify large network modifications, and local information to identify loss of generation or islanded operation.

This paper proposes a model-adaptive relay that continuously adapts the relay settings based on the network configuration and the available short-circuit current. The main novelty of the proposed model adaptive relay is that it continuously runs a short-circuit study to programmatically calculate the relay setting. The short-circuit study is based on the results obtained from a power system model which runs locally on an Field Programable Gate Array (FPGA) in real time. The fault current from the model is then used for the adaptive algorithm to calculate the relay settings, considering coordination with the downstream fuses and upstream reclosers. The power system model is updated through a communication network (DNP3 or Modbus) to capture the status of field devices, such as reclosers and online generators. This automatization simplifies the programming of the relays while also eliminating the need of multiple settings groups, which is typically four to seven in commercial protective devices. This methodology is scalable and can calculate the settings for complex networks with multiple Distributed Energy Resources (DERs) in the system.

TABLE I: ADAPTIVE PROTECTION METHODS

Approach	Approach
Communication-less approach [11]	• Uses local information to adapt to operation mode (grid, island, meshed, radial and the disconnection of some DGs). • Loss of generation with subsequent relay configuration based on different reclosing times. • Uses anti-islanding capability of relays to change between operation modes. • Relay settings are calculated offline and updated in an online mode.
Communication-less [10]	• Detects island or grid condition or loss of generation using only local information • Uses relay anti-islanding algorithms to change states between grid connected and islanded mode • Changes pickup setting to adapt to different states • Limited to three phase faults • This method needs knowledge of the initial grid state (grid-connected/island/generation)
Hybrid [12]	• Central controller adapts settings for large network reconfigurations • Local information is used to adapt settings based on IBRs status (Online/Offline) • Two-stage protection approach is proposed. 1) Offline fault analysis is first done to compute relays settings for every possible operating mode, which are then stored in respective relay memories. 2) In second stage, an online state detection algorithm is implemented to detect the operating state of the network. Thereafter, the relays adopt appropriate settings as per identified network.
Communication based [13]	• Use communication to change group settings depending on the MG configuration • The status of the microgrid is detected by the operation of the main switch that connects the utility-grid to the microgrid and transferred to the relays by a communication link • Different settings for the overcurrent relays are calculated offline and saved in relays.
Communication-less [14]	• Communication assisted • Provides protection for both modes of operation and does not require communication. • It applies the definite-time grading technique; it can take a relatively long time to isolate a fault within a large medium-voltage microgrid, particularly in the islanded mode of operation

II. Case Study Microgrid Protection

This section presents simulation results that showcase the challenges of implementing overcurrent protection schemes in inverter-based microgrids. A real microgrid located in Chattanooga, Tennessee is used as a case study to illustrate the challenges of microgrid protection using overcurrent elements. The Simulink model of the microgrid is presented in Fig 1. The microgrid operates at 12.47 kV and consists of 1.3 MW of PV generation and 1 MWh of energy storage. The islanding operation is enabled by a Tesla Megapack, which regulates the voltage and frequency of the microgrid. The fault current of the energy storage inverter is not public, and is assumed to be 2.0 p.u. The PV inverter is programmed to limit its current to 1.0 p.u. The feeders are protected by 30 T, 50 T, and 100 T ampere-rated fuses. The substations have Schweitzer Engineering Laboratories (SEL)- microgrids 751 protective relays, and S&C IntelliRupters installed along the 12.47 kV distribution lines that can detect different types of faults in the system.

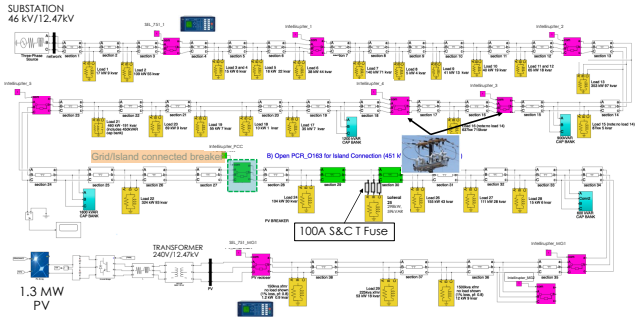

Figure 1: Field microgrid. Green dashed line encloses the microgrid.

Fig. 2 shows the current time-inverse curves for the 100 A fuse and the IntelliRupter that protects the feeder. This IntelliRupter protects the microgrid using two profiles, one for grid tied and another for islanded operation. The IntelliRupter uses U4

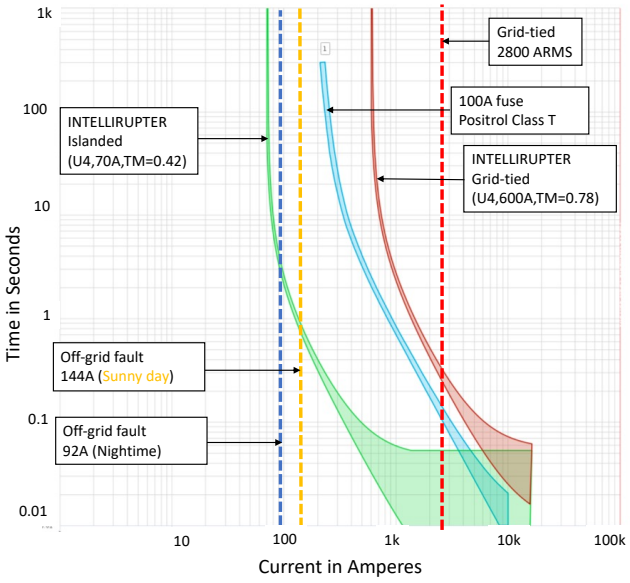

Figure 2: TCC curves for lateral protected with 100A fuse

curves for both profiles. For the grid-tied operation, the pick-up current is 600 A with a time dial (TD) of 0.78. For islanded operation, the pickup current is 70 A with a TD=0.42.

To showcase the challenges of protecting a lateral power line with fuses in microgrids, a three-phase fault was introduced in lateral 25, which is protected by a 100 A fuse. During grid-tied application, the substation provides high fault current (2800 A), and the fault is quickly cleared by the fuse in less than 0.04 s. However, during islanded operation, the maximum combined fault contribution from the PV inverters and the energy storage is 144 A. As shown in Fig. 2., because of this low short-circuit current the fuse won't clear the fault. To solve this problem, the utility configured the IntelliRupter to trip at very low current. Although this protection scheme will isolate the fault, tripping the IntelliRupter would leave the entire microgrid without power.

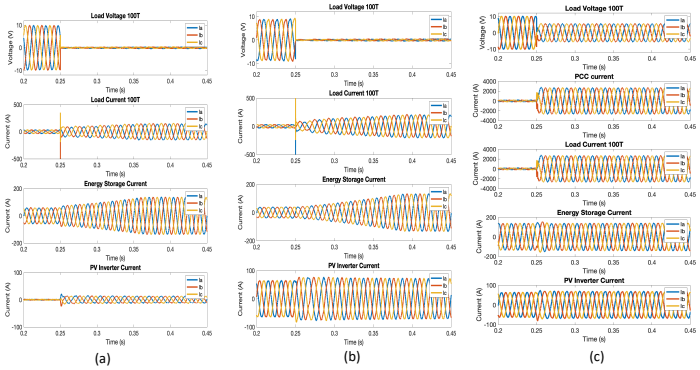

Figure 3: (a) Islanded mode low-irradiance day. (b) Islanded mid-irradiance. (c) Islanded mode high irradiance.

Fig. 3. Shows the simulated current waveforms from the ES and PV inverters when a three-phase fault is introduced at t=0.25 s in the lateral 25. As seen in the figure, the three-phase fault causes an immediate current pulse of short duration, which is caused by the passive inductive loads in the microgrid. The short-circuit surge decays in less than 40 μs and has no significant energy to be useful for protection purposes. During the fault, the current control of the PV inverter regulates the current to be 1.0 p.u., which is set by the saturation of the dc link control loop. In the same figure, notice that the irradiance influences the available fault contribution from the PV. For very low irradiance (less than 100 W/m^2), the fault contribution from the PV inverters is very small. However, the fault contribution from the PV inverter remains at 1.0 p.u. for irradiances greater than (500 W/m^2).

III. Model-Adaptive Relay Working Principles

This section presents the model-adaptive relay, its operation and building blocks. Fig. 4 shows the main modules of the model-adaptive relay: I) Real-time power system simulator. II) Communication module. III) Short-circuit analysis module. IV) Relay module. All these modules run on a single Kyntex-7 FPGA included in the NI-CRIO 9039.

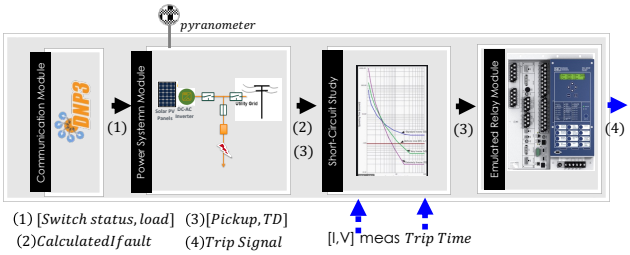

Figure 4: Model adaptive relay modules

A. Real-Time power system model

The power system model runs the following models in real time on LabView FPGA: I) PV inverter, including controls and average model of the power converter. II) physics-based model of PV farm, III) Impedance LR line sections. The substation is modelled as a three-phase grid in series with an LR section. The equations of the three-phase PV inverter with connection to the grid, with the average state model and the external elements of the circuit are given by equations (1.1) and (1.2).

$$\begin{bmatrix} v_a \\ v_b \\ v_c \end{bmatrix} = L\frac{d}{dt}\begin{bmatrix} i_a \\ i_b \\ i_c \end{bmatrix} + R\begin{bmatrix} i_a \\ i_b \\ i_c \end{bmatrix} + \begin{bmatrix} d_a \\ d_b \\ d_c \end{bmatrix} v_{dc} \tag{1.1}$$

$$\frac{d}{dt}v_{dc} = \frac{1}{C}(I_{DCPV} - I_{DC}) \tag{1.2}$$

Where i_{abc} are the inverter output currents, v_{abc} the voltage at the point of connection, d_{abc} the duty cycle, L and R the grid filter inductance and resistance, v_{dc} the DC-link voltage I_{DCPV} the PV panel output current and I_{DC} the inverter DC current.

The control for the PV inverter is designed using (1.3) and (1.4).

$$\frac{\tilde{\imath}_d}{\tilde{d}_d} = \frac{V_{dc}}{(sL_d + r)} \tag{1.3}$$

$$\frac{\tilde{\imath}_q}{\tilde{d}_q} = \frac{V_{dc}}{(sL_q + r)} \tag{1.4}$$

LR line section has as an input the voltage at the input terminal of the inductor V_{Lin}, the current through the inductor I_L, the inductance resistance r_L, and the inductance L in Henries. The output voltage is calculated trough (1.5):

$$V_{out} = V_{Lin} - r_L I_L - \frac{dI_L}{dt}L \tag{1.5}$$

The physics-based PV array model is described by the following equations

$$I = I_{PV} - I_0\left[exp\left(\frac{V + R_s I}{V_t a}\right) - 1\right] - \frac{V + R_s I}{R_{\_}} \tag{1.6}$$

Where I_{pv} and I_0 are the photovoltaic and saturation currents of the array and $V_t = N_s kT/q$ is the thermal voltage of the array with N_s cells connected in series. If the array is composed of N_p parallel connections of cells the photovoltaic and saturation currents may be expressed as: $I_{pv} = I_{pv,\,cell} N_p, I_0 = I_{0,\,cell} N_p$. R_s is the equivalent series resistance of the array and R_p is the equivalent parallel resistance [15].

B. Short-Circuit Study Module

This module receives the maximum short-circuit current from the power system module and the instantaneous load from the communication module. The pickup is calculated by multiplying the load by a constant σ. To maintain coordination, the adaptive relay receives the trip time at the available fault current from the upstream recloser and downstream fuses. Finally, the user specifies the desired trip time for the relay $t(s)$. This information is fed into (1.6), which is the IEC TCC curve, which is used to calculate the Time Multiplier Setting (TMS). The TMS and pickup are the settings to be programmed in the relay to determine the TCC curve. The protection philosophy is to guarantee the user specified trip time regardless of the available short-circuit current.

$$TMS = \left. t(s)\left(\left(\frac{I}{\sigma I_{load}}\right)^{\alpha} - 1\right)\right/_{k} \tag{1.6}$$

Where σ is set to 1.25, α=2 and k=80 to represent the IEC extremely inverse curve.

C. Field Deployment Package

Fig. 5 (c) shows the field deployment package of the model-adaptive relay. The package consists of 1) CRIO 9039, 2) Uninterruptable Power Supply. 3) Industrial computer, which is the gateway for remote access. 4) G&W Rogowski coils which provide the current measurements and voltage measurements for the model-adaptive relay. Fig. 5 (d) shows a 3D aerial representation of the model adaptive relay installation.

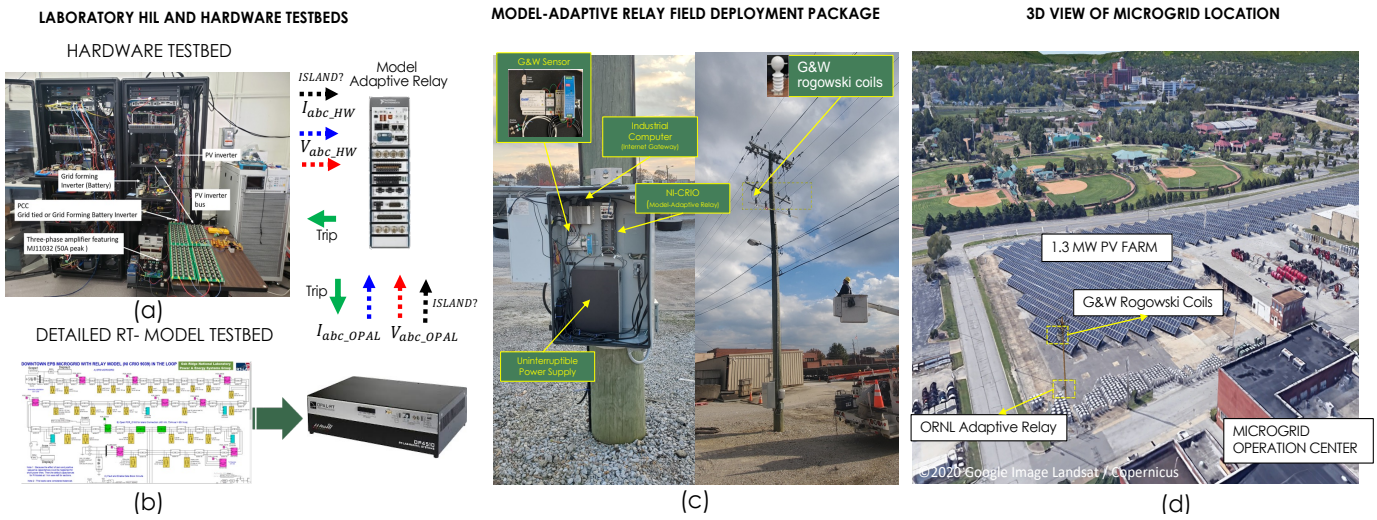

Figure 5: Laboratory testing and field deployment of the model-adaptive relay (a) hardware testbed. (b) HIL testbed (c) field deployment

III. Experimental Results

Fig. 6 shows the TCC curves for the upstream and downstream fuses protecting a line lateral, as well as the curves calculated by the model-adaptive relay. Two fault current contributions are evaluated (140 A and 300 A), and for two pickup currents 50A and 70A. The 144A current is the fault current during islanded mode on a sunny day. The 300A is the contribution when the diesel backup generator is online. The pickup reflects changes in the load during the day. For this example, the user established a trip time of 0.8 seconds. This information is used together with the available fault current and the pickup to calculate the TMS. The grading time to maintain fuse-relay coordination is set 0.3s. As seen in the figure, the model adaptive relay adjusts the TCC curves based on the available generation and load in the lateral. Regardless of the generation, the trip time for all cases 0.8s. Notice that for the grid-tied operation, the adaptive relay is programed as a fuse-blow scheme.

Fig. 7 (a,b) shows HIL and experimental results for the model-adaptive relay when operating in islanding mode and grid-tide mode. Fig. 7(c,d) shows the experimental results from the hardware testbed when the relay operates in island and grid-tied mode. These graphs include the dq control signals of the PV inverter and the DC-link voltage response during the fault.

The HIL setup used for this study is shown in Fig. 5(b), which consists of an Opal-RT 4510 running the full microgrid model. The hardware setup, shown in Fig. 5(a), is a low voltage testbed that incorporate power hardware-in-the-loops models to emulate PV inverters, diesel generators, energy storage devices and wind turbines. For this test, only the grid, the PV inverter and ESS were emulated. The measurements were multiplied by scaling factors to match the simulated microgrid power rating. More details about this testbed can be found here [16,17].

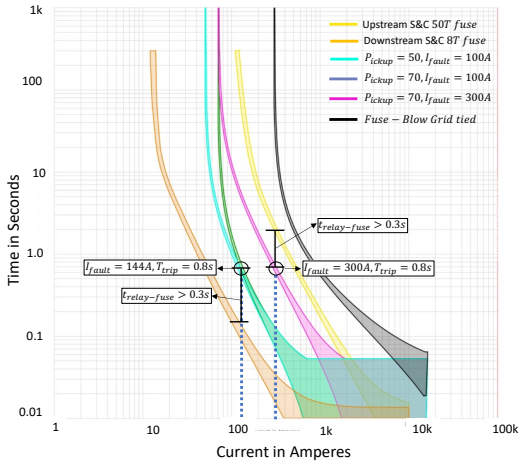

Figure 6: Model-Adaptive relay adapting TCC curves based on

In Fig. 7(a) a three-phase fault was applied at t=5.0s during islanded operation. Running in the background, the adaptive relay receives the status of the PCC switch and based on the available generation, determines the settings of the relay. For this test, the available fault current is 144A and the breaker trips in 0.8s, as specified by the user. Fig. 7(c) shows the same three phase fault applied in the hardware testbed. Notice that control signals of the PV inverter have similar dynamics to that in simulation. Similarly, the breaker tripped in 0.8s. Fig. 7(b) show the HIL results when the microgrid is grid-tied. For this experiment, the model-adaptive relay changes to a fuse-blow scheme and the trip time corresponds to the 50A fuse protecting the lateral as the grid provides a large fault contribution and the 50T fuse clears after just 0.02 seconds. Fig. 7(d) shows the results obtained from the hardware testbed. Because the grid emulator in the hardware testbed has thermal limitation the available fault current is limited. During grid tied operation, the fuse takes more time to blow and finally opens in 0.16s. For this case the model-adaptive relay was also set in the fuse-blow scheme.

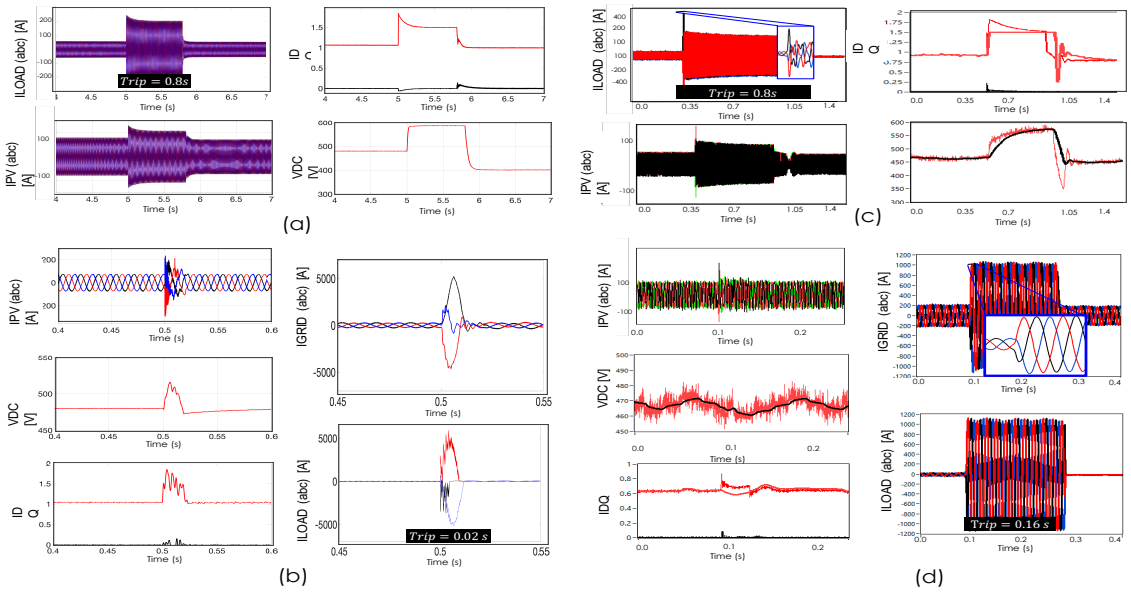

Figure 7: Laboratory testing of the model-adaptive relay. (a) Island mode HIL, (b) grid tied HIL, (c) Island hardware, (d) grid tied hardware.

IV. Conclusions

This paper proposes a model-adaptive relay that continuously adapts the relay settings based on the network configuration and the available short-circuit current. The presented model-adaptive relay is composed of a real-time power system simulator, a communication module, and a short-circuit analysis module, which continuously run to programmatically adjust the TCC curves in the relay. This automatization simplifies the programming of the relays while also eliminating the need of multiple settings groups. This methodology is scalable and can calculate the settings for complex networks with multiple distributed DERs in the system.

It was demonstrated through experimental and hardware-in-the-loop results, that the proposed model-adaptive relay effectively protected the laterals against short-circuit faults in the microgrid during islanded operation. The future work includes additional protection elements, such as sequence components and voltage elements, to further increase the selectivity and sensitivity of the proposed method.

Acknowledgment

This work was accomplished thanks to the collaborations with Jim Glass, Manager of Smart Grid Developments at the Electric Power Board (EPB) of Chattanooga, and G&W Electric Company.

References

[1] A. Hooshyar and R. Iravani, "Microgrid Protection," in Proceedings of the IEEE, vol. 105, no. 7, pp. 1332-1353, July 2017, doi: 10.1109/JPROC.2017.2669342.

[2] S. H. Horowitz and A. G. Phadke, *Power System Relaying*, 3rd ed. New York, NY, USA: Wiley, 2008.=

[3] L. Che, M. Khodayar, and M. Shahidehpour, "Adaptive protection system for microgrids: Protection practices of a functional microgrid system," *IEEE Electrific. Mag.*, vol. 2, no. 1, pp. 66–80, Mar. 2014.

[4] T. S. Ustun, C. Ozansoy, and A. Zayegh, "Modeling of a centralized microgrid protection system and distributed energy resources according to IEC 850-7-420," *IEEE Trans. Power Syst.*, vol. 27, no. 3, pp. 1560– 1567, Aug. 2012.

[5] H. H. Zeineldin, H. M. Sharaf, D. K. Ibrahim and E. E. A. El-Zahab, "Optimal Protection Coordination for Meshed Distribution Systems With DG Using Dual Setting Directional Over-Current Relays," in IEEE Transactions on

[6] S. Gonzalez, N. Gurule, M. J. Reno and J. Johnson, "Fault Current Experimental Results of Photovoltaic Inverters Operating with Grid- Support Functionality," 2018 IEEE 7th World Conference on Photovoltaic Energy Conversion (WCPEC) (A Joint Conference of 45th IEEE PVSC, 28th PVSEC & 34th EU PVSEC), Waikoloa Village, HI, 2018, pp. 1406-1411.

[7] N. S. Gurule, J. Hernandez-Alvidrez, M. J. Reno, A. Summers, S. Gonzalez and J. Flicker, "Grid-forming Inverter Experimental Testing of Fault Current Contributions," 2019 IEEE 46th Photovoltaic Specialists Conference (PVSC), Chicago, IL, USA, 2019, pp. 3150-3155.

[8] S. Chowdhury, S.P. Chowdhury, P. Crossley, Microgrids and active distribution networks, in: IET Renewable Energy Series 6, The Institution of Engineering and Technology, London, United Kingdom, 2009.

[9] M. Khederzadeh "Adaptive setting of protective relays in micro-grids in grid-connected and autonomous operation," in *Proc. IET International Conf. on Developments in Power System Protection*, 2012, pp. 1- 4.

[10] P.Mahat,Z.Chen,B.Bak-Jensen,andC.Bak,"Asimpleadaptiveover- current protection of distribution systems with distributed generation," *IEEE Trans. Smart Grid*, vol. 2, no. 3, pp. 428–437, Sep. 2011.

[11] C. Liu, Z. Chen and Z. Liu, "A communication-less overcurrent protection for distribution system with distributed generation integrated," 2012 3rd IEEE International Symposium on Power Electronics for Distributed Generation Systems (PEDG), 2012, pp. 140-147, doi: 10.1109/PEDG.2012.6253992.

[12] B. P. Bhattarai, B. Bak-Jensen, S. Chaudhary and J. R. Pillai, "An adaptive overcurrent protection in smart distribution grid," 2015 IEEE Eindhoven PowerTech, 2015, pp. 1-6, doi: 10.1109/PTC.2015.7232310.

[13] M. Khederzadeh "Adaptive setting of protective relays in micro-grids in grid-connected and autonomous operation," in *Proc. IET International Conf. on Developments in Power System Protection*, 2012, pp. 1- 4.

[14] M. A. Zamani, A. Yazdani, and T. S. Sindhu, "A communication-assisted protection strategy for inverter based medium voltage micro-grids," *IEEE Trans. Smart Grid*, vol. 3, pp. 2088-2099, Dec. 2012.

[15] M. G. Villalva, J. R. Gazoli and E. R. Filho, "Modeling and circuit-based simulation of photovoltaic arrays," *2009 Brazilian Power Electronics Conference*, 2009, pp. 1244-1254, doi: 10.1109/COBEP.2009.5347680.

[16] M. Ferrari, B. Park and M. M. Olama, "Design and Evaluation of a Model-Free Frequency Control Strategy in Islanded Microgrids with Power-Hardware-in-the-Loop Testing," *2021 IEEE Power & Energy Society Innovative Smart Grid Technologies Conference (ISGT)*, 2021, pp. 1-5, doi: 10.1109/ISGT49243.2021.9372219.

[17] M. Ferrari, E. C. Piesciorovsky, T. Smith and J. Hambrick, "Cost-Effective Three-Phase Current Amplifier Interface for Real-time Simulator with Relays in-the-Loop," *2019 North American Power Symposium (NAPS)*, 2019, pp. 1-5, doi: 10.1109/NAPS46351.2019.9000320.